Journal of Alloys and Compounds 506 (2010) 575–580

Contents lists available at ScienceDirect

Journal of Alloys and Compounds

journal homepage: www.elsevier.com/locate/jallcom

Electrochemical corrosion behavior in NaCl medium of zinc–nickel alloys electrodeposited under applied magnetic field

S. Chouchane[a], A. Levesque[b,*], P. Zabinski[c], R. Rehamnia[a], J.-P. Chopart[b]

[a] Faculté des Sciences, Université Badji Mokhtar, Annaba, Algeria
[b] LACM-DTI URCA, BP 1039, 51687 Reims Cedex 2, France
[c] Physical Chemistry and Electrochemistry Laboratory, Faculty of Non-Ferrous Metals, AGH University of Science and Technology, 30-059 Krakow, Poland

ARTICLE INFO

Article history:
Received 27 April 2010
Received in revised form 12 July 2010
Accepted 12 July 2010
Available online 17 July 2010

Keywords:
Zn–Ni alloy
Magnetic field
Corrosion
NaCl solution
AFM

ABSTRACT

The electrochemical codeposition of zinc–nickel alloy coatings from sulfate bath has been carried out under low and high applied magnetic field. The influence of alloy structural parameters upon corrosion behavior is discussed. It has been found that the magnetically induced convection modifies the phase composition, promoting the zinc phase in spite of the γ-Ni_5Zn_{21}. Low magnetic field acts also on the morphology of the deposits by reducing the grain size and the average roughness R_a. For alloy obtained with low magnetic field superimposition, surface morphology modification has no significant effect on corrosion behavior whereas for low nickel content alloy, the modification of phase composition, induced by applied magnetic field, favours higher polarization resistance. When high magnetic field amplitude is involved, the phase composition modifications are the same that for low applied B and the morphology is not largely modified. In this case, the hydrogen reduction current dramatically decreases that leads to a large shift of the corrosion potential. It is suggested that the surface reactivity of electrodeposited alloys depends on the magnetically induced convection that is efficient during the codeposition process.

1. Introduction

Electrodeposited coatings of zinc–nickel alloys have attracted much attention because they possess higher corrosion resistance and better mechanical characteristics than pure zinc or other zinc-alloys [1–8]. Actually, zinc–nickel alloys are considered as having the potential to replace the cadmium in anticorrosion applications and have found wide applications in automobile, electronic or other industries [9]. The coatings must be sacrificial in relation with substrate; therefore, the choice of substitution metals is governed by their position on the corrosion potential scale in NaCl environment. Several authors show that Zn–Ni alloys have the best corrosion behavior in saline environment [10–12]. The corrosion resistance of alloys depends practically on the percentage of Ni atoms. According to some reports, an alloy composition including 10–15 at% of nickel leads to a maximum corrosion resistance [13,14]. However, many other parameters could modify the corrosion behavior such as morphology, or crystallographic phase composition. Albalat et al. found that the presence of particular additives in the electrolyte media improved the surface homogeneity, which leads to better corrosion resistance even for an alloy with low Ni content [15]. The single phase structure usually observed in these alloys with 13 at% of nickel is the γ-Ni_5Zn_{21} phase. Ramanauskas suggested that the metal structural parameters were responsible for the properties of the thin passive or thick protective film on the surface. The crystal structure can affect thickness, composition, adhesion or solubility of the film on the metal surface [7].

A way to obtain different composition phases of alloys is to superimpose a magnetic field during codeposition process [16–29]. When an electrochemical codeposition is undertaken under magnetic field, convection in the electrolytic solution is induced: it is the so-called MHD effect (magneto-hydrodynamic effect). Fahidy reported that surface roughness decrease could be induced by MHD effects on the surface three-dimensional deposit film structure [20]. Devos et al. reported that a magnetic field could change the surface morphology and the preferred orientation of the nickel grain due to an increase of the diffusion flux of specific inhibiting species [22]. Our previous papers have shown that low magnetic field reduces the surface roughness and that structural changes could be observed for zinc–nickel alloys electrodeposited under applied magnetic field [30,31]. The aim of this work was to study the zinc–nickel alloy behavior in NaCl solution in order to evaluate the link between the applied magnetic effect which induces changes on morphology and structure, and the corrosion behavior. Therefore zinc–nickel alloy coatings have been characterized by using AFM, X-ray diffraction and EDS. Corrosion behavior has been studied by

* Corresponding author. Tel.: +33 3 26 91 33 50; fax: +33 3 26 91 89 15.
E-mail address: alexandra.levesque@univ-reims.fr (A. Levesque).

0925-8388/$ – see front matter © 2010 Elsevier B.V. All rights reserved.
doi:10.1016/j.jallcom.2010.07.099

Table 1
Bath chemical compositions for zinc–nickel alloy codeposition.

Bath names	$C_{Ni^{2+}}$ (mol L^{-1})	$C_{Zn^{2+}}$ (mol L^{-1})	$C_{Ni^{2+}}/C_{Zn^{2+}}$
S_1	0.20	0.60	0.33
S_2	0.50	0.60	0.83
S_3	0.70	0.60	1.17

means of polarization curves which have been obtained in thermostated 3% NaCl solution without superimposition of magnetic field.

2. Experimental

The samples were prepared by electrochemical codeposition with respectively horizontal low ($B \leq 1$ T) and vertical high ($B \leq 12$ T) superimposed magnetic field. For the first case, experiments have been undertaken by means of an electromagnet (DRUSCH EAM 20 G), for high magnetic field, we have used the facilities of the Grenoble High Magnetic Field Laboratory (CNRS). For all experiments, the magnetic field was constant and uniform on the electrode surface and in the vicinity (diffusion layer) of the electrode. The working electrode was directed horizontally or vertically according to the field direction in order to be parallel to the field. To prepare the solutions, the following salts have been used: $ZnSO_4{\cdot}7H_2O$, $NiSO_4{\cdot}7H_2O$ and H_3BO_3 (40 g L^{-1}). The chemical compositions of the used electrolytes are given in Table 1. The pH was adjusted by addition of few droplets of sulfuric acid in order to perform the Zn–Ni alloy at pH = 2.5 and the bath temperature was kept constant at 25 °C. The codeposition apparatus has been already described as well as the experimental procedure in our previous papers [30,31]. The working electrode (WE) was a 1 cm^2 Ti disk, embedded in epoxy resin. To avoid epitaxial phenomenon, the titanium was oxidized in H_2O_2 before each codeposition process. The deposition of Ni–Zn was performed at a constant applied potential equal to $E = -1750$ mV *vs.* saturated mercury sulfate (SSE) reference electrode and a Pt counter electrode was used. The amounts of zinc and nickel which were deposited were negligible compared to the amounts of zinc and nickel ions in solution, therefore, these last quantities can be regarded as constant for each codeposition experiment.

An X-ray diffractometer (Bruker D8 Advance) with a Cu monochromatic radiation ($\lambda = 1.54056$ Å) was used to determining phase composition of the alloys. The chemical composition and surface morphology have been characterized by scanning electron microscopy (SEM) (JEOL JSM 6460LA microscope coupled with an EDS JEL 1300 microprobe), and atomic force microscopy (AFM) (System Ntegra Prima). AFM studies were carried out at atmospheric pressure and room temperature in contact mode. Images were obtained with the same micro-lever; thus the obtained average roughness (R_a) parameters can be compared for different samples.

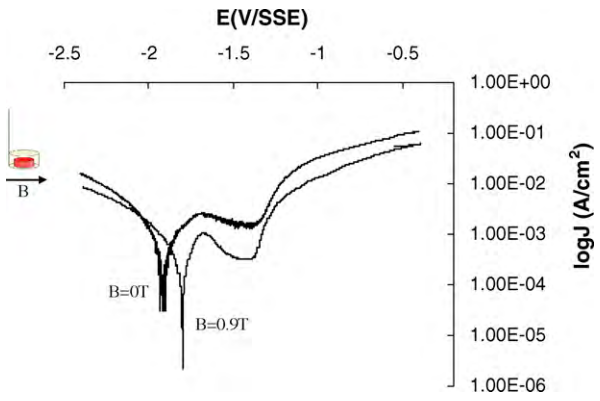

Fig. 2. Polarization curves of Zn–Ni coatings realized at $C_{Ni^{2+}}$ equal to 0.5 M without and with applied magnetic field equal to 0.9 T in 3% NaCl solution.

Corrosion tests were carried out in a NaCl environment at 3% without superimposed magnetic field. The corroding medium was not deaerated by bubbling of inert gases before or during electrochemical tests. All polarization curves have been performed by potential linear voltammetry using potentiostat/galvanostat (PGZ 301, Radiometer). Curves have been obtained with a sweep rate equal to 2 mV/s, the scanning range was −0.5 to 0.5 V from the open circuit potential that has been measured during 4 min before performing the polarization curve. The counter electrode was a platinum foil and a saturated calomel electrode (SCE) was used as reference electrode. The electrochemical measurement data were analyzed by Voltamaster 4 electrochemical software.

3. Results and discussion

3.1. Low applied magnetic field

Figs. 1–3 show respectively the anodic and cathodic polarization curves obtained in 3% NaCl solution on zinc–nickel coatings. The deposits have been obtained for different concentrations of nickel ions, $C_{Ni^{2+}}$, with a constant zinc ion concentration, $C_{Zn^{2+}} = 0.6$ M in the electrolytic bath. The E_{corr} corrosion potential and R_p polarization resistance are reported in Table 2 for deposits that have

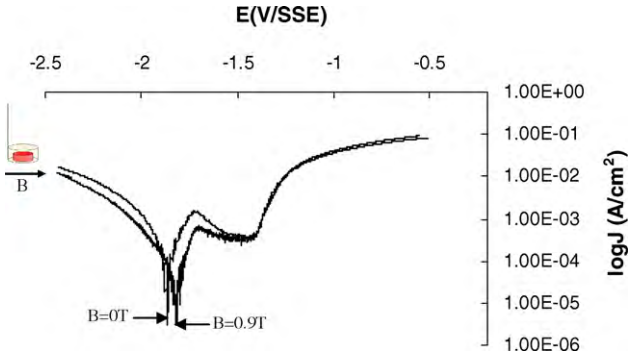

Fig. 1. Polarization curves of Zn–Ni coatings realized at $C_{Ni^{2+}}$ equal to 0.2 M without and with applied magnetic field equal to 0.9 T in 3% NaCl solution.

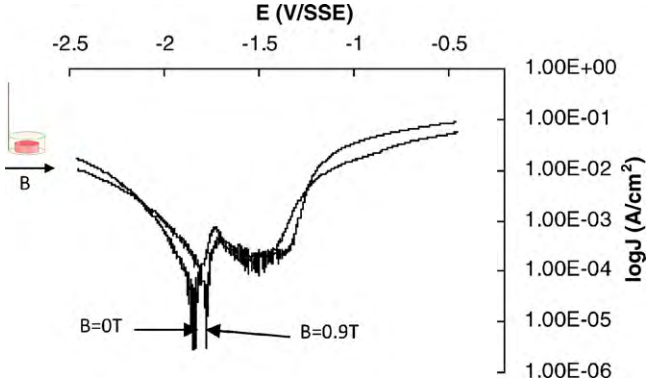

Fig. 3. Polarization curves of Zn–Ni coatings realized at $C_{Ni^{2+}}$ equal to 0.7 M without and with applied magnetic field equal to 0.9 T in 3% NaCl solution.

Table 2
Rest potential and polarization resistance at rest potential of alloys as a function of B and nickel concentration in the bath $C_{Ni^{2+}}$.

$C_{Ni^{2+}}$ (mol L^{-1})	E_{corr} (V)			R_p (Ω cm^2)		
	$B = 0$ T	$B = 0.9$ T[a]	$B = 12$ T	$B = 0$ T	$B = 0.9$ T	$B = 12$ T
0.2[a]	−1.87	−1.82		159	504	
0.5[a]	−1.91	−1.81		78	125	
0.7[a]	−1.83	−1.78		430	256	
0.7[b]	−1.38		−1.52	360		1450

[a] Magnetic field and downward electrode are horizontal.
[b] Magnetic field and electrode are vertical.

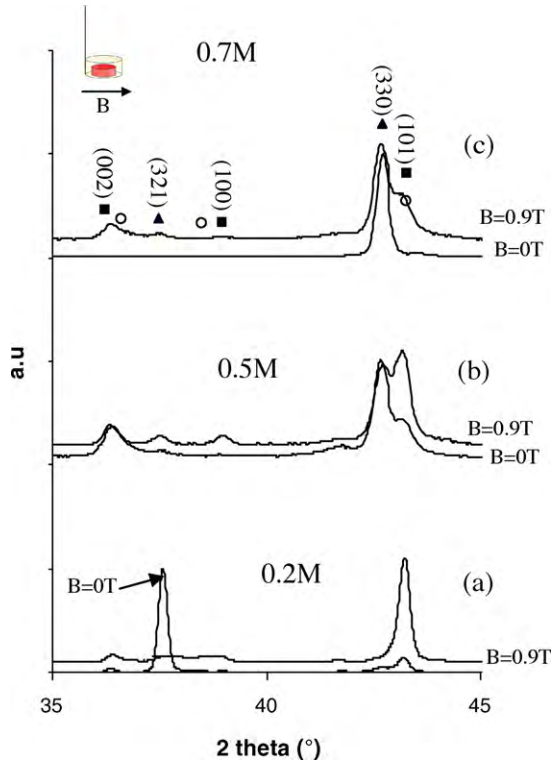

Fig. 4. X-ray diffraction patterns of Zn–Ni alloy under applied magnetic field $B = 0$ and 0.9 T for different $C_{Ni^{2+}}$ (○ η-phase, ▲ γ-Ni_5Zn_2, ■ Zn).

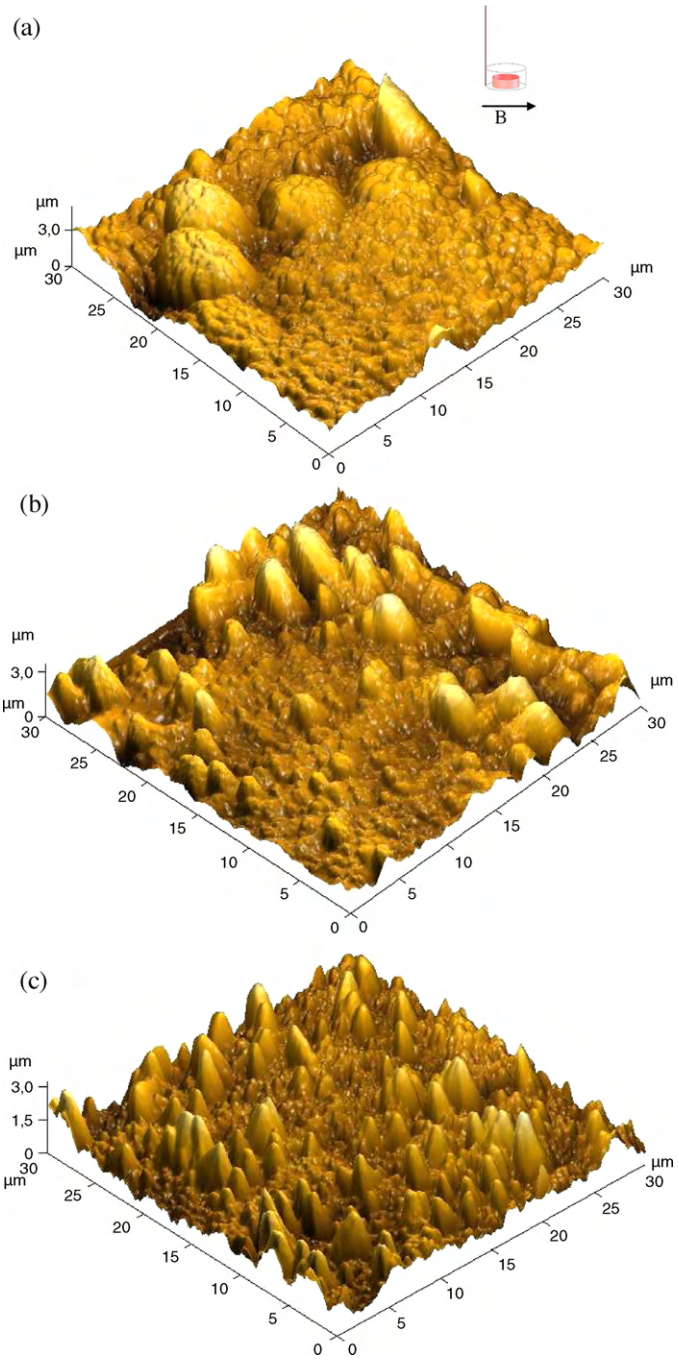

Fig. 5. AFM images of Zn–Ni alloys deposits at $C_{Ni} = 0.7$ M for different applied magnetic fields (a) $B = 0$ T, (b) $B = 0.45$ T and (c) = 0.9 T. The scan area is 30 μm × 30 μm.

been realized with a low horizontal magnetic field applied on a horizontal electrode facing down. The corrosion potential of the coating deposited under low magnetic field moved positively, compared with the coating obtained without B which indicates that the magnetic field is helpful to reducing thermodynamic tendency of corrosion. This effect of magnetic field is the same for all concentrations $C_{Ni^{2+}}$. However, the corrosion resistance of the coating is mainly determined by the polarization resistance or corrosion current. The coating with low nickel content in the alloy (0.2 and 0.5 M of nickel ions in the electrolyte bath) showed a best corrosion resistance when magnetic field was applied during the electrodeposition process. For the alloy realized with 0.7 M of nickel ions, the magnetic field had not improved the corrosion resistance. It was already demonstrated that for zinc based alloy coatings the corrosion behavior depends on texture, stress in the coating, phase composition and chemical composition [32–35]. In our case, this behavior induced by B, cannot be attributed to the variation of the chemical composition because as it has been shown in previous paper, the magnetic field affects the composition crystallographic phase and the morphology of the alloy but, whatever applied magnetic field, the chemical composition of the alloy does not change [30]. The X-ray diffraction patterns of Zn–Ni alloys have been performed before they were immerged in NaCl bath and are presented in Fig. 4. For different $C_{Ni^{2+}}$, the alloys are a mixture of zinc, η and γ-phase structure. The magnetic field favours the (1 0 1) orientation of zinc phase. For 0.2 M (Fig. 4a), the (3 2 1) γ-phase disappears and the η and zinc phases are favoured. For 0.5 M (Fig. 4b), the (3 3 0) γ-Ni_5Zn_{21} and the zinc phases are present without magnetic field. When the magnetic field is applied, the Zn phase is promoted compared to the (3 3 0) γ-Ni_5Zn_{21} orientation. For $C_{Ni^{2+}}$ equal to 0.7 M (Fig. 4c), without magnetic field, only the (3 3 0) γ-Ni_5Zn_{21} can be detected but with superimposition of a magnetic field, once more, the (1 0 1) orientation of zinc phase is promoted. The phase composition varies on the same way when magnetic field is applied regardless the nickel ion concentration $C_{Ni^{2+}}$. Magnetic field always favours the zinc and η phases.

Table 3
Nodule size and roughness R_a obtained by AFM measurement.

%at of Ni in alloy	B (T)	Nodule size (μm)	R_a (nm)
5–7	0	2.111	435
5–7	0.45	0.925	445
5–7	0.9	0.760	374
13	0	2.323	425
13	0.45	1.379	184
13	0.9	1.246	159

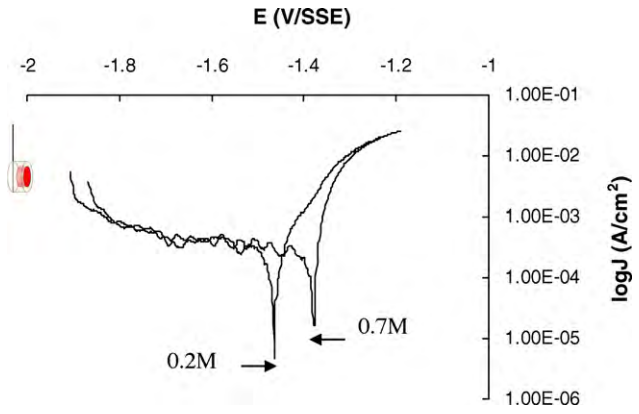

Fig. 6. Polarization curves of Zn–Ni coatings realized at different $C_{Ni^{2+}}$ 0.7 and 0.2 M for horizontal and vertical working electrode in 3% NaCl solution.

In case of 0.2 and 0.5 M, the zinc and η phases are always detected with and without applied magnetic field. Generally, simultaneous presences of these phases do not improve the corrosion resistance. It has been reported that coatings from acid bath were thought to be a mixture of η-phase and γ-phase structures [33]. Due to the fact that potentials of these two phases are different, a corrosion cell tends to be formed in corrosive environments and therefore, these coatings may exhibit generally lower corrosion protection. However, in previous studies [30,31], we have shown that the solubility of Ni in Zn crystals increases with magnetic field. This phenomenon allows keeping the same atomic ratio of Ni in the coating whereas the deposit becomes less rich in the phase γ-Ni_5Zn_{21}. The solid solution of zinc which contains more nickel when magnetic field is applied could be more efficient against corrosion in NaCl solution. It could be one of the explanations for the higher polarization resistance of the low nickel content alloy obtained when magnetic field is applied during the electrochemical codeposition process.

For $C_{Ni^{2+}}$ equal to 0.7 M (13 at% of Ni in alloy) and without magnetic field, only the (3 3 0) γ-Ni_5Zn_{21} can be detected but with an applied magnetic field, the (1 0 1) orientation of zinc phase is again promoted and the γ-Ni_5Zn_{21} is always detected. Park et al. have demonstrated that formation of the dual phase η + γ in alloys with about 15 at% of nickel is responsible for an increase of the corrosion current. They also observed that zinc–nickel coatings that consist of η single phase and a nickel content of 13–15% have better corrosion resistance than the coatings that consist of the γ secondary phase

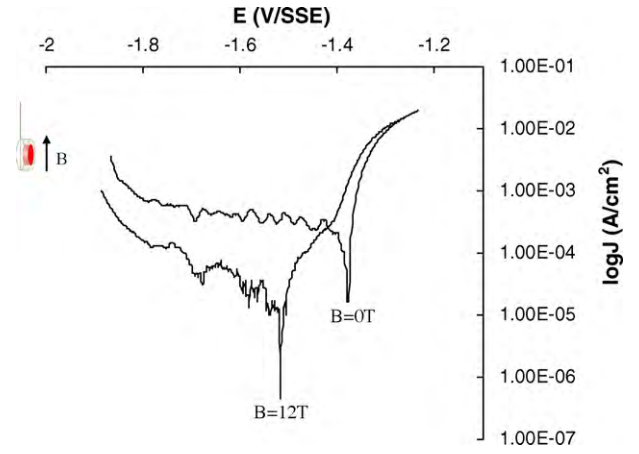

Fig. 7. Polarization curves for the deposits at C_{Ni} = 0.7 M prepared under magnetic field in NaCl solution at 3%.

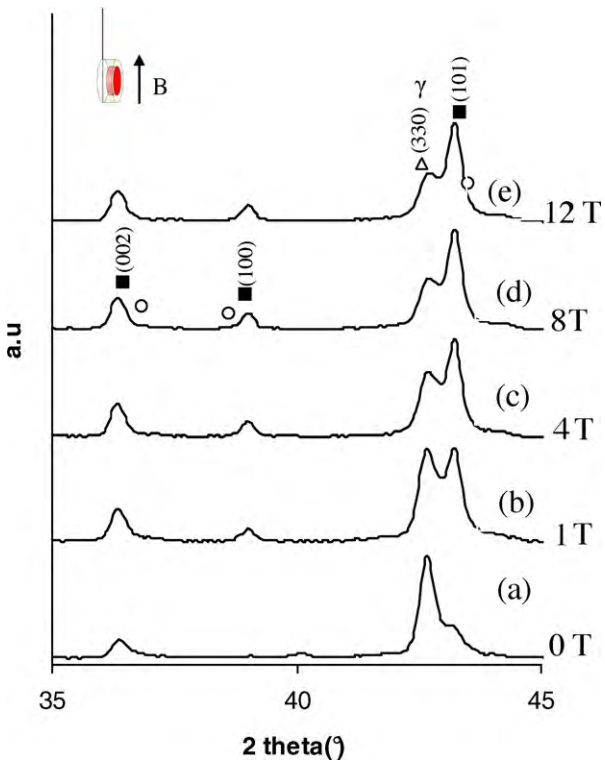

Fig. 8. X-ray diffraction patterns of Zn–Ni alloys at pH 2.5 with magnetic field at concentration: $C_{Zn^{2+}}$ = 0.6 M; $C_{Ni^{2+}}$ = 0.7 M (■ Zn, △ γ-Ni_5Zn_{21}, ○ η-phase).

and have higher than 15% nickel content [34]. Byk et al. reported that the zinc–nickel coating consisting of Ni_5Zn_{21} phase exhibits the best corrosion protective properties in a chloride environment [35]. This is in good agreement with former results [36,37,39]. In our study, the same result is observed for alloys with a content of nickel equal to 13 at%: magnetic field favours the presence of the dual phases and the polarization resistance is affected by applied magnetic field.

From observations of the influence of surface morphology on the corrosion behavior, it is suggested that the initial surface morphology of coatings plays an important role in improving the corrosion resistance of alloys. Generally, the roughness factor describes the initial surface irregularity. Rough surfaces expose more weakly bonded sites and exhibit higher dissolution rates. The morphology of the Zn–Ni coating elaborated with magnetic field is different from those obtained without applied magnetic field. AFM images of coatings are presented in Fig. 5a–c. The sample with about 13 at% of Ni, performed without B, exhibits a nodular coarse-grained morphology whereas the nodules are finer for B = 0.9 T. For these samples, the AFM measurements confirm that size of nodules decreases from 2.32 to 1.25 μm respectively without and with applied magnetic field (Table 3). The same behavior has been also observed by Scanning Electronic Microscopy in previous paper for low Ni content Zn alloy [30]. In addition, zinc–nickel alloy surface is less rough when a magnetic field is superimposed. The average roughness (R_a) of an alloy containing 13 at% of Ni was 425 nm whereas with a magnetic field at 0.9 T, this parameter is equal to 159 nm. The magnetic field allows obtaining finer nodules and less rough surface [28,42] which could promote better behavior in NaCl media according different studies [40,41]. The nodule size decreases for all nickel concentrations in the electrolyte bath; we can suggest that this phenomenon does not govern the corrosion resistance.

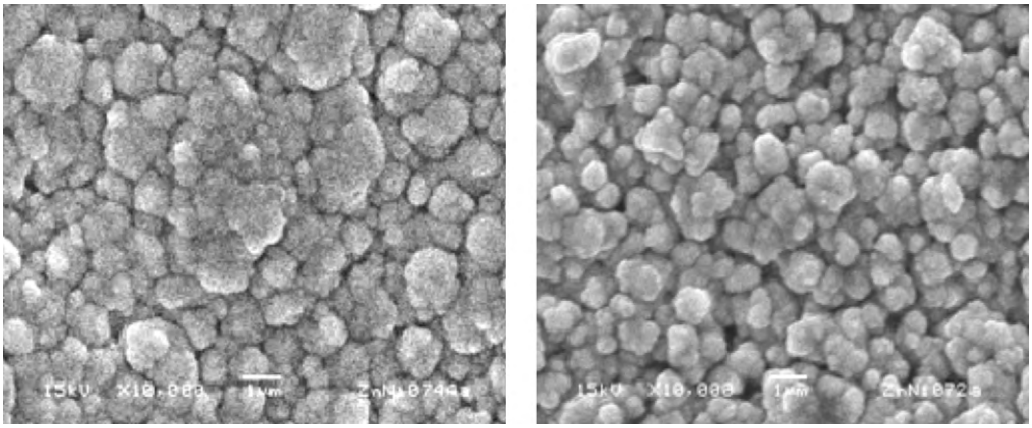

Fig. 9. SEM images of Zn–Ni alloy deposits at $C_{Ni^{2+}} = 0.7$ M for different applied magnetic fields (a) $B = 0$ T and (b) $B = 12$ T.

3.2. High applied magnetic field

Some electrodeposits have been obtained with high vertical magnetic field up to 12 T. In order to be in a configuration similar to low magnetic field experiments, namely magnetic field parallel to the working electrode, the electrode has to be used in vertical position.

Fig. 6 shows the polarization curves of alloys obtained for vertical working electrode in NaCl solution for $C_{Ni^{2+}}$ equal to 0.7 and 0.2 M without magnetic field. For both nickel concentrations in the electrolyte bath, the corrosion potential is more positive for the vertical orientation of the working electrode than for the horizontal one (Figs. 1 and 3). This first observation highlights the role of electrode orientation, i.e. the role of the natural convection. Thus, for both orientations, the alloys with high content of nickel present more nobler corrosion potential in agreement with numerous studies [10,12–14] and no geometrical surface effect can be highlighted since the anodic and cathodic plateau currents are the same in both cases.

The polarization curves are presented in Fig. 7 for alloys obtained with magnetic field up to 12 T in vertical mode. The cathodic part of polarization curve is significant. Potentials are shifted to cathodic values, in the same time the cathodic current density of corrosion decreases for the deposits. The polarization resistance is largely higher for the deposit realized with an applied magnetic field equal to 12 T (Table 2). It is important to notice that, in this case, the chemical composition does not vary with the magnetic field amplitude. This induced inhibiting effect reveals a magnetic field capability on materials that can be very useful to get new properties by magnetic processes.

When magnetic field was applied up to 12 T for $C_{Ni^{2+}}$ equal to 0.7 M, the intensity of the (3 3 0) γ-Ni_5Zn_{21} peak decreased and the (1 0 1) zinc orientation (Fig. 8) was favoured. The same phenomenon was observed for low magnetic field. However, the behavior in NaCl media is not the same for low magnetic field regarding to higher one. For low magnetic field, the potentials are shifted to more positive values and no difference in cathodic current density can be observed with B. X-ray diffraction patterns of Zn–Ni alloys obtained without magnetic field, for the two configurations, reveal different phase compositions (Fig. 4c and Fig. 8a). In the case of vertical working electrode, the alloy consists of two phases: zinc or η and γ-Ni_5Zn_{21} whereas the horizontal one consists only of the γ-Ni_5Zn_{21}. Previous study has demonstrated that the alloys obtained in vertical mode contain an amount of nickel equal to about 9 at% and could explain the difference for the crystallographic phase composition. Chemical and phase compositions of alloys obtained with high magnetic field are the same than those obtained with low magnetic field at 0.5 M of $C_{Ni^{2+}}$ (Fig. 4b). Therefore, the difference of alloy behavior in NaCl does not seem to be actually linked with phase composition.

The morphology of alloys has been studied by scanning electron microscopy. As it can be seen in Fig. 9, the morphology of the deposit is not significantly different between the deposits realized with and without applied magnetic field. The fact that the anodic currents for higher potential values are equal is evidence that the real surfaces of the deposits are not modified and therefore the effect that is highlighted does not depend on morphological phenomenon.

These results are evidence that magnetic field in vertical mode has an effect on alloy corrosion. Due to the fact that the phase composition also varies with B, the relation between corrosion behavior and phase composition of the alloys is not clear. So, we can assume that the shift in the potential will be binded to other parameters like microstructure which could be induced by the amplitude of B and working electrode configuration, these other parameters induce modifications on the reactivity of the surface toward the hydrogen evolution since the cathodic current is largely decreasing for the alloy electrodeposited with high magnetic field superimposition. This magnetically induced effect on surface reactivity can be very useful for catalytic or synthesis purposes and has to be investigated in more detail.

4. Conclusion

A constant and uniform magnetic field superimposed on the electrochemical cell in a direction parallel to the working electrode provokes some modifications on the phase composition and morphology of zinc–nickel alloys. Corrosion of zinc–nickel alloys electrodeposited under magnetic field superimposition has been investigated with low and high magnetic field amplitude. The corrosion behavior has been studied in sodium chloride solution without superimposed magnetic field; that means that the results are only depending on the electrodeposited zinc–nickel alloy. The main result is that magnetic field can significantly improve the corrosion resistance of alloys with low alloy nickel content. When the horizontal magnetic field has a low amplitude ($B < 1$ T), the induced deposit roughness modification has no important effect on the corrosion behavior of the electrodeposited zinc–nickel alloy whereas the induced phase composition modification improves the polarization resistance of alloys which contain about 5 at% of nickel.

When high magnetic field amplitude is involved, the morphology is not largely modified but the hydrogen reduction current dramatically decreases that leads to a large shift of the corrosion potential. This phenomenon is evidence for magnetic effect on the

surface reactivity of electrodeposited alloys and has to be deeply analyzed by further researches.

Acknowledgments

Authors thanks the financial support of the European Commission from the 6th framework programme "Transnational Access – Specific Support Action" contract N° RITA-CT-2003-505474, Champagne-Ardenne Region for financial support and the Laboratoire National des Champs Magnétiques Intenses (CNRS) for helpful assistance. This work is realized within the framework of GDRE GAMAS.

References

[1] C. Müller, M. Sarret, M. Benballa, Electrochim. Acta 46 (18) (2001) 2811.
[2] J.B. Bajat, Z. Kacarevie-Popovie, V.B. Miskovie, M.D. Maksimovie, Prog. Org. Coat. 39 (2000) 127.
[3] R. Ramanauskas, L. Muleshkova, L. Maldonado, P. Dobrovolskis, Corros. Sci. 40 (1998) 401.
[4] R. Fratesi, G. Rovinti, Surf. Coat. Technol. 82 (1996) 158.
[5] Z. Zhou, T.J. O'Keefe, Surf. Coat. Technol. 96 (1997) 191.
[6] M.R. Kalantary, G.D. Wilcox, D.R. Gabe, Electrochim. Acta 40 (1995) 1609.
[7] R. Ramanauskas, Appl. Surf. Sci. 153 (1999) 53.
[8] Z. Wu, L. Fedrizzi, P.L. Bonora, Surf. Coat. Technol. 85 (1996) 170.
[9] CEE Recommendation (Directive du Conseil de la Communauté Européenne) n° 91/338/CEE, 1991.
[10] M. Gavrila, J.P. Millet, H. Mazille, D. Marchandise, J.M. Cuntz, Surf. Coat. Technol. 123 (2000) 164–172.
[11] K.R. Baldwin, M.J. Robinson, C.G.E. Smith, Corros. Sci. 36 (1994) 1515.
[12] L. Felloni, R. Frastesi, E. Quadrini, G. Roventi, J. Appl. Electrochem. 17 (1987) 574.
[13] G.D. Wilcox, D.R. Gabe, Corros. Sci. 35 (1993) 1251.
[14] N. Gage, D.A. Wright, Proc. Asia Pacific Interfinish 90, Singapore, 19–22 November, 1990, pp. 65–71.
[15] R. Albalat, E. Gomez, C. Muller, J. Pregonas, M. Sarret, E. Vallès, J. Appl. Electrochem. 21 (1991) 44.
[16] K.H. Lee, J. Yoo, J. Ko, H. Chung, D. Chang, et al., Phys. C 372 (2002) 866.
[17] A. Rucinskiene, G. Bikulcius, L. Gudavicuite, E. Juzelias, Electrochem. Commun. 4 (2002) 86.
[18] H.R. Khan, K. Petrikowski, Mater. Sci. Forum 373 (2001).
[19] C. O'Reilly, G. Hinds, J.M.D. Coey, J. Electrochem. Soc. 148 (2001) C674.
[20] T.Z. Fahidy, Prog. Surf. Sci. 68 (2001) 155.
[21] S. Bodea, L. Vignon, R. Ballou, P. Molho, Phys. Rev. Lett. 83 (1999) 267.
[22] O. Devos, A. Olivier, J.P. Chopart, O. Aaboubi, G. Maurin, J. Electrochem. Soc. 145 (1998) 401.
[23] D.Y. Li, J. Appl. Electrochim. Acta 42 (1997) 37.
[24] A. Chiba, T. Ogawa, T. Yamshita, Surf. Coat. Technol. 34 (1988) 455.
[25] R. Aogaki, K. Fueki, T. Makaido, Denki Kagaku 44 (1976) 89.
[26] L. Yang, J. Electrochem. Sci. 101 (1954) 456.
[27] J.C. Shannon, Z.H. Gu, Z.T. Fahidy, J. Electrochem. Soc. 145 (1998) L314.
[28] A. Krause, C. Hamann, M. Uhlemann, A. Gebert, L. Schultz, J. Magn. Magn. Mater. 290 (2005) 261.
[29] A. Krause, M. Uhlemann, A. Gebert, L. Schultz, Electrochim. Acta 49 (2004) 4127.
[30] S. Chouchane, A. Levesque, J. Douglade, R. Rehamnia, J.P. Chopart, Surf. Coat. Technol. 201 (2007) 6212.
[31] A. Levesque, S. Chouchane, J. Douglade, R. Rehamnia, J.P. Chopart, Appl. Surf. Sci. 255 (2009) 8048.
[32] G.Y. Li, J.S. Lian, L.Y. Niu, Z.H. Jiang, Surf. Coat. Technol. 191 (2005) 59.
[33] E. Beltowaska-Lehaman, P. Ozga, Z. Swiatek, C. Lupa, Cryst. Eng. 5 (2002) 335.
[34] H. Park, J.A. Szpunar, Corros. Sci. 40 (1998) 525.
[35] T.V. Byk, T.V. Gaevskaya, L.S. Tsybulskaya, Surf. Coat. Technol. 202 (2008) 5817.
[36] R. Ramanauskas, P. Quintana, L. Maldonado, R. Pomés, M.A. Pech-Canul, Surf. Coat. Technol. 92 (1997) 16.
[37] V. Raman, M. Pushpavanam, B.A. Shenoi, Met. Finish. 81 (1983) 85.
[39] R. Ramanauskas, Appl. Surf. Sci. 153 (1999) 53–64.
[40] M.E. Vela, G. Andreasen, S.G. Aziz, R.C. Salvarezza, A.J. Arvia, Electrochim. Acta 43 (1998) 3.
[41] M.G. Fernandes, R.M. Latanision, P.C. Searson, Phys. Rev. B 47 (1993) 11749.
[42] K. Msellak, J.P. Chopart, O. Jbara, O. Aaboubi, J. Amblard, Magnetohydrodynamics 39 (2003) 487.